# Analysis of the Performances of Organic Light-Emitting Devices with a Doped or an Undoped Polyaniline–Poly(4-styrenesulfonate) Hole-Injection Layer

**Anna De Girolamo Del Mauro,[1] Giuseppe Nenna,[1] Valentina Bizzarro,[2] Immacolata Angelica Grimaldi,[1,3] Fulvia Villani,[1] Carla Minarini[1]**

[1]*Italian National Agency for New Technologies, Energy and the Environment, UTTP, Nanomaterials and Device Technology Section, Portici Research Center, Piazzale E. Fermi 1, 80055 Portici (Naples), Italy*
[2]*IMAST Portici, Piazzale E. Fermi, 80055 Portici (Naples), Italy*
[3]*Department of Physics, University of Naples "Federico II," V. Cintia 1, 80126 Naples, Italy*

Received 28 April 2011; accepted 28 April 2011
DOI 10.1002/app.34773
Published online 10 August 2011 in Wiley Online Library (wileyonlinelibrary.com).

**ABSTRACT:** Transparent and conductive nanocomposite films were spin-coated with the use of undoped and dimethyl sulfoxide (DMSO)-doped polyaniline (PANI)–poly(styrene sulfonate) (PSS) dispersions. The prepared dispersions were investigated in terms of their nanoparticle size distributions, and the corresponding films were morphologically, optically, and electrically characterized. These films were used as hole-injection layers (HILs) in organic light-emitting diode (OLEDs), and the device performances were compared to a reference device without an HIL. The device based on the PANI–PSS layer showed the best electrooptical characteristics, lowest switch-on voltage, and improved efficiency. In particular, the device efficiency grew about three times with the introduction of the PANI–PSS layer (1.20 Cd/A) and about two times with the introduction of the DMSO-doped PANI–PSS film (0.77 Cd/A) compared to an OLED without an HIL (0.4 Cd/A). These results indicate that the device with the undoped PANI–PSS was the more suitable one to be used as an HIL in an OLED device. © 2011 Wiley Periodicals, Inc. J Appl Polym Sci 122: 3618–3623, 2011

**Key words:** conducting polymers; light-emitting diodes (LED); nanoparticles

## INTRODUCTION

Organic light-emitting diodes (OLEDs) have attracted great attention as potential flat panel displays, thanks to their outstanding advantages, such as wide viewing angle, fast response, and easy fabrication and processing. Many efforts have been made to improve the device structures and to understand their working mechanism. In OLEDs, the injection efficiency is a critical parameter, which depends, to a large extent, on the work function of the electrode. The potential barrier between indium thin oxide (ITO) and the adjacent organic layer severely limits the efficiency of the hole injection. Mechanical polishing, chemical solvents, or dry cleaning and surface functionalization have been applied to ITO to control the hole-injection ability and to improve the performances of OLEDs.[1]

A lot of work has also been devoted to the anode buffer layers placed between ITO and the organic material[5–10] to improve the electroluminescence (EL) efficiency and to reduce the driving voltage. Different materials, such as copper–phthalocyanine,[11] polyaniline (PANI),[12] poly(3,4-ethylene dioxythiophene) (PEDOT),[13] platinum,[14] carbon,[15] silicon nitride,[16] 4,4V,4W-tris(3-methylphenylphenylamino) triphenylamine,[17] Ni-ITO co-sputtered layer,[18] and metal oxides,[19] have been investigated for insertion between the ITO anode and the hole-transporting layer to enhance the EL efficiency, to increase the stability, and to lower the driving voltage of OLEDs.

Among the aforementioned materials, PANI is regarded as one of the most favored conductive polymers for several electrochemical and electronic applications, thanks to its high electrical performance, easy conductivity control, thermal stability, and easy handling.[20]

The blending of PANI with poly(styrene sulfonate) (PSS) was already carried out,[21] and they showed good compatibility to each other; this blending resulted in a material with good capability of processing by melt or solution and with a moderate conductivity.

*Correspondence to:* A. De Girolamo Del Mauro (anna.degirolamo@enea.it).

Contract grant sponsor: Technology and Research for the Application of Polymer in Electronic Devices (TRIPODE) project financed by the Ministero dell'Universita' e della Ricerca; contract grant number: DM 20160.

To improve the electrical conductivities, conductive polymers are exposed to selective reagents through a process known as *secondary doping*,[22–24] and the mechanism that rules the conductivity enhancement, thanks to the exposures to seemingly unrelated solvents, remains controversial.[23,24] For example, when PEDOT–PSS, namely, a commercial PEDOT template synthesized with poly(styrene sulfonic acid), is exposed to sorbitol, dimethyl sulfoxide (DMSO), or even ethylene glycol, its electrical conductivity can be improved by two orders of magnitude.[25]

Although conductivity enhancement was demonstrated with secondary PANI doping with small acid molecules with exposure to select solvents,[22,26] in the literature, there are no reports concerning the use of DMSO as a solvent for the doping of PANI–PSS with the aim of increasing its electrical conductivity.

In this study, OLEDs with a PANI–PSS nanocomposite layer, used as a polymeric hole-injection material, were manufactured, and the effects of the undoped and DMSO-doped PANI–PSS layers on the performances of the OLEDs were investigated by comparison of the electrooptical properties of these devices with the ones of the EL devices fabricated without a hole-injection layer (HIL). The morphology and the electrical conductivity of both the undoped PANI–PSS and DMSO-doped PANI–PSS films were also investigated to carefully examine the function of these layers in the optoelectronic device.

## EXPERIMENTAL

### Synthesis

PSS (weight-average molecular weight = 70,000), aniline monomer, ammonium persulfate, and hydrochloric acid (HCl) were purchased from Aldrich (Warrington, UK) and were used without further purification.

Water-dispersed PANI–PSS was synthesized by the chemical oxidation polymerization of aniline in the presence of excess HCl according to a method reported in literature.[27] Therefore, 50 μL of aniline monomer was mixed with 40 mL of deionized water and 7.3 mL of an HCl (0.5*M*) aqueous solution. Successively, the aqueous PSS solution (0.6 g) was added to the mixed solution and was stirred for 1 h. The polymerization of the aniline was performed with ammonium persulfate (0.1575 g) as an oxidizing agent for 12 h at 0°C. During the polymerization, the aniline monomers were linked to the relatively long PSS chains because of the electrostatic interactions between the negatively ionized sulfonic acid and the positively ionized anilinium ions and formed emeraldine-salt-type PANI segments (short polymer chains or oligomers). These polymer complexes became entangled with each other and formed nanoparticles as a final result.

After the polymerization, a dark green PANI–PSS nanoparticle solution was obtained. Dark green is the characteristic color of the conductive emeraldine salt form of PANI.

The water-dispersed PANI–PSS and DMSO-doped PANI–PSS were used as HILs in OLED devices. The DMSO-doped PANI–PSS dispersion was prepared by mixture of the PANI–PSS dispersion with 5 wt % DMSO. The mixed solution was filtered and continuously stirred for 12 h at room temperature before it was deposited by spin-coating.

### Device fabrication

Commercial ITO-coated glass (Delta Technologies, Loveland, CO) was used as the substrate. The ITO sheet resistance was 4–10 Ω/sq. The substrates were cleaned by sequential rinsing in nonionic detergent and boiling in deionized water for 2 h in an ultrasonic bath with isopropyl alcohol for 10 min and were dried under a nitrogen flow. Then, the substrate was treated with an oxidizing piranha solution ($H_2SO_4/H_2O_2$) for 15 min, rapidly withdrawn from the solution, rinsed with deionized water, and blown dry with $N_2$ gas. This procedure created a hydrophilic surface to improve the interfacial adhesion of the PANI–PSS dispersions with the ITO surface. Before deposition, the PANI–PSS dispersion was filtered through a 0.45-μm poly(vinyl difluoride) filter to remove the bigger aggregates. Both the PANI–PSS and DMSO-doped PANI–PSS dispersions were spin-coated on the patterned ITO substrates by means of a Brewer Science model 100 spin coater. Finally, the samples were baked at 80°C for 30 min in a vacuum oven.

OLED devices with a three-layer structure were fabricated. The EL device stack consisted of an HIL, with PANI–PSS or DMSO-doped PANI–PSS, an *N*,*N*′-di-{[(1-naphthyl)-*N*,*N*′-diphenyl]-1,1-biphenyl)}-4,4′-diamine (NPD) hole-transporting layer, and an electron-transporting and emitting layer of aluminum tris(8-hydroxyquinoline) ($Alq_3$) material. The three organic layers were sandwiched between a transparent ITO anode and a lithium fluoride (LiF)/aluminum (Al) cathode, as schematized in Figure 1(b).

For comparison, a device with the structure without the HIL was also manufactured [Fig. 1(a)].

The small molecule organic layers and the cathode films were deposited by thermal evaporation in a high-vacuum chamber ($10^{-7}$ mbar base pressure). The active area of the devices was 1.27 $\times$ $10^{-5}$ $m^2$.

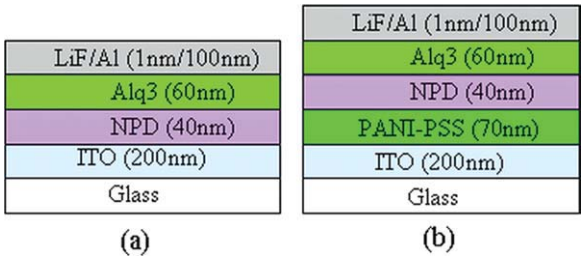


**Figure 1** Schematic section of the OLED stacks. [Color figure can be viewed in the online issue, which is available at wileyonlinelibrary.com.]

## Characterization

The PANI–PSS dispersions were investigated by dynamic laser scattering (DLS) analysis with an HPPS 3.1 system (Malvern Instruments, Worcestershire, UK) to determine the particle size distribution in suspension and the dispersion stability in the solutions.

A profilometer (TENCOR P10 surface profiler, KLA Tencor, Milpitas, CA) was used to measure the thickness of the deposited films.

The synthesized PANI–PSS was investigated through Fourier transform infrared (FTIR) spectroscopy analysis (Nicolet 380 FTIR system, Thermo Fischer, Waltham, MA). The analyzed samples were prepared from the PANI–PSS aqueous solution and precipitated with excess ethanol with the aim of obtaining the solid form of PANI–PSS. A small amount of PANI–PSS powder was ground with KBr and made into a pellet. The FTIR spectrum was detected in the absorption mode.

The morphology of the PANI–PSS films without and with DMSO was analyzed by a scanning electron microscope (LEO 1530, Carl Zeiss S.p.A., Peabody, MA) and by atomic force microscopy (AFM; Veeco, Dimension Digital Instruments Nanoscope IV, Plainview, NY) in tapping mode.

The transmittance of the films deposited on the glass/ITO substrate was measured by means of a UV–visible spectrophotometer (PerkinElmer Lambda 900).

The electrical conductivity of the films was measured with a four-point probe system (Napson Co., Chiba City, Japan).

Current voltage (*I–V*) measurements were performed with a Keithley 2400 power supply source meter in voltage mode (Cleveland, OH), with constant increment steps and a delay time of 1 s before each measurement point. An integrating sphere and a calibrate photodiode (Newport 810UV, Irvine, CA) connected to a Keithley 6517A electrometer were employed for the EL analysis.

All of the characterizations was performed in air at room temperature.

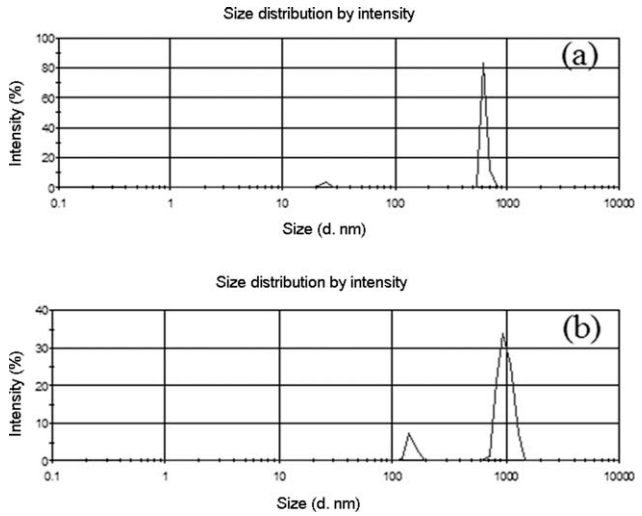


**Figure 2** DLS distribution of the (a) PANI–PSS and (b) DMSO-doped PANI–PSS dispersions.

## RESULTS AND DISCUSSION

The distribution, average size, and dispersion stability in the PANI–PSS and DMSO-doped PANI–PSS dispersions were measured through DLS analysis. The DLS values indicated that the PANI–PSS dispersion was characterized by two narrow peaks centered at about 25 and 600 nm [Fig. 2(a)], whereas the DLS curve related to the DMSO-doped PANI–PSS dispersion had two peaks at 140 and 900 nm.

This analysis indicated that the doping increased the size of the PANI–PSS particles, an opposite effect with respect to the one observed in PEDOT–PSS, where the nanoparticle size decreased from 444 to 27.6 nm after DMSO modification.[28]

No precipitate was observed in the resultant PANI–PSS and DMSO-doped PANI–PSS dispersions after an aging time of 4 months, thanks to the strong electrostatic interaction between PANI and PSS.

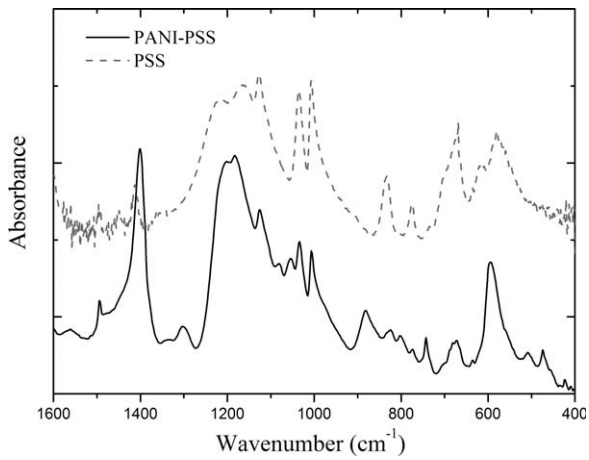


**Figure 3** FTIR spectra of the (a) PSS and (b) PANI–PSS powder pellets.

**TABLE I**
**Assignments of FTIR Bands to PSS and PANI–PSS and Related Intensity Values**

| Assignment | PSS ($cm^{-1}$) | PANI–PSS ($cm^{-1}$) |
|---|---|---|
| Symmetric stretching of the $SO_3H$ group | 1183 | 1183 |
| In-plane skeleton vibration of the benzene ring | 1129 | 1124 |
| $SO_2$ stretching | 1035 | 1035 |
| In-plane bending vibration of the benzene ring | 1011 | 1006 |
| C—S stretching of the benzene ring of PSS | 671 | 674 |

The FTIR measurements (Fig. 3) were performed to verify that the prepared films consisted of PANI and PSS. Indeed, the presence of the characteristic PSS peaks in the FTIR spectrum of the PANI–PSS film demonstrated that the polymerization was successful.[29] The main absorption peaks were assigned, and the related intensity values are reported in Table I.

The AFM analysis was performed on the PANI–PSS and DMSO-doped PANI–PSS films spin-coated on a glass substrate. The results (Fig. 4) show that the morphology of the investigated samples was very dissimilar, and the surface root-mean-square roughness values resulting were 10 nm for PANI–PPS and 13.1 nm for DMSO-doped PANI–PSS. In particular, the roughness was expected to play an important role in the device efficiency, as indicated in previously studies.[30] Indeed, the lower roughness value of HIL led to enhanced device performance because a more flat surface allowed a more uniform conducting path for holes to migrate across the ITO/HIL and HIL/hole transport layer (HTL) interfaces.

The PANI–PSS (50 nm) and DMSO-doped PANI–PSS (55 nm) films spin-coated on the glass/ITO substrate appeared colored and transparent [Fig. 5(a)]. The transmission spectra of the glass/ITO substrate and glass/ITO/PANI–PSS (50 nm) are shown in Figure 5(b). The DMSO-doped PANI–PSS spectra is not reported because it was very similar to the PANI–PSS one. The spectrum analysis indicated high transmittance values in the visible wavelength range for the prepared samples. In particular, at $\lambda = 600$ nm, where the human eye is very sensitive, the transmittance of the glass/ITO/PANI–PSS stack was 84.1%,

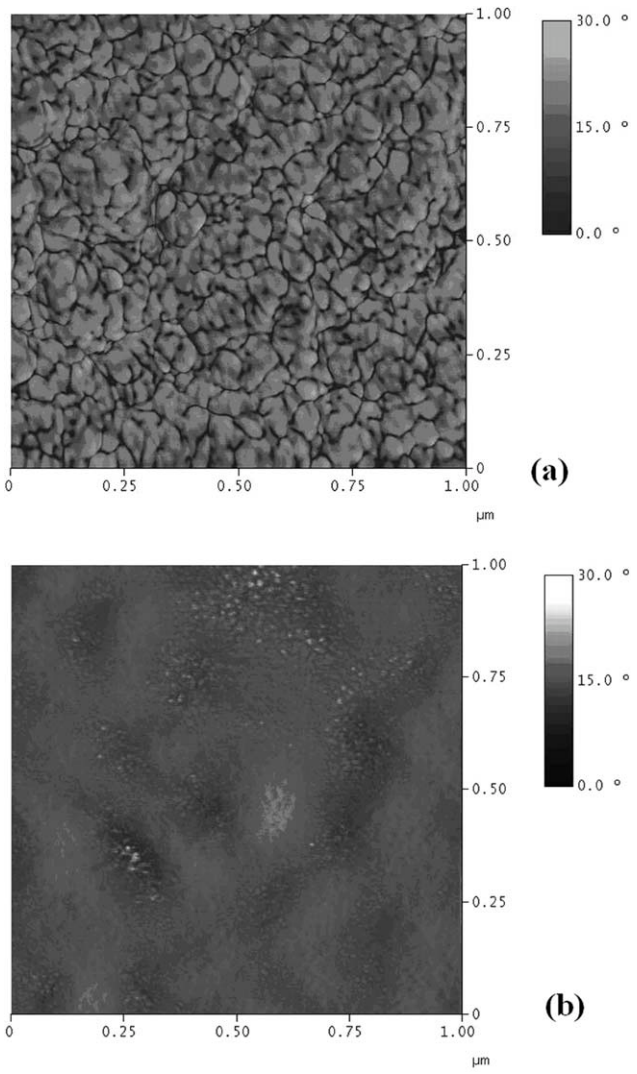


**Figure 4** AFM phase images of the (a) PANI–PSS and (b) DMSO-doped PANI–PSS nanocomposite films.

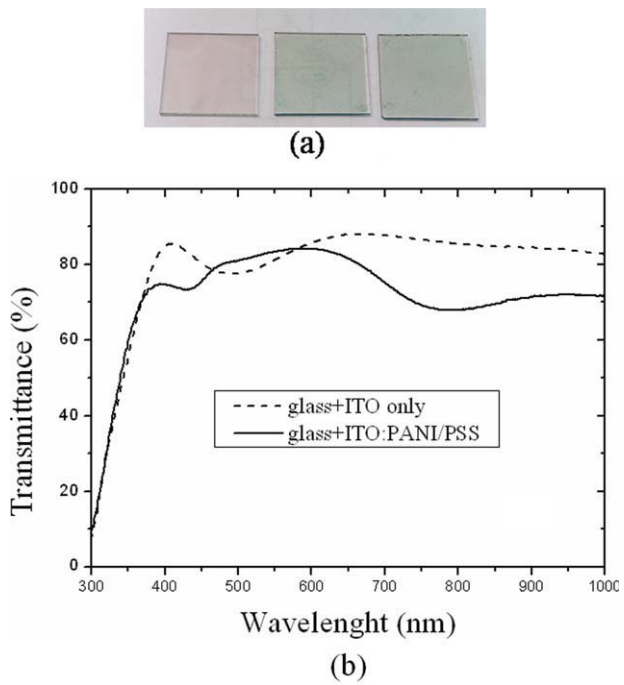


**Figure 5** (a) Pictures (from left to right) of glass/ITO, glass/ITO/PANI–PSS, and glass/ITO/DMSO-doped PANI–PSS and (b) transmittance spectra of the glass/ITO/PANI–PSS and of the glass/ITO systems. [Color figure can be viewed in the online issue, which is available at wileyonlinelibrary.com.]

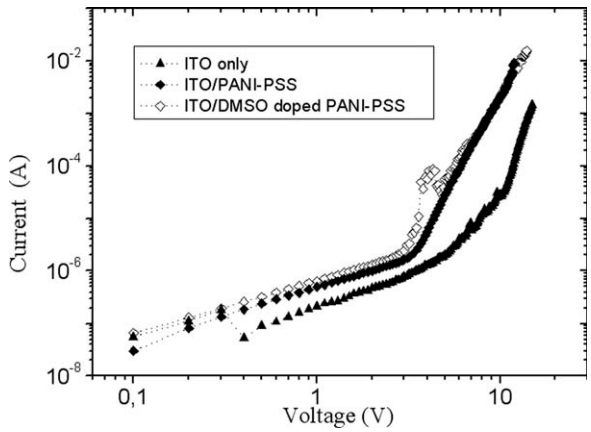


**Figure 6** *I–V* curves of the devices with ITO/PANI–PSS, ITO/DMSO-doped PANI–PSS, and only ITO.

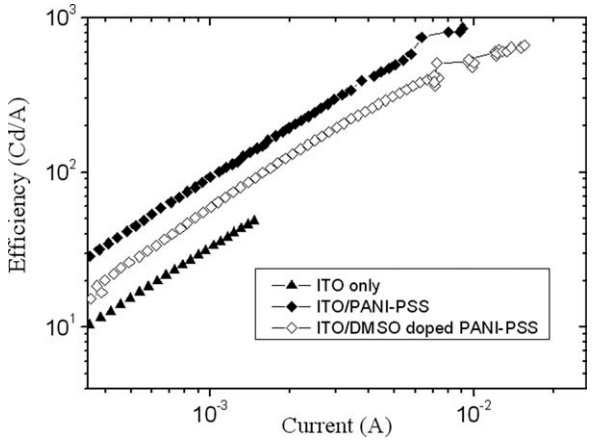


**Figure 8** Efficiency of OLED devices with ITO/PANI–PSS, ITO/DMSO-doped PANI–PSS, and only ITO.

compared to that of the glass/ITO one with a value of 86%. This indicated that the insertion of the PANI–PSS film as an HIL in the OLED structure did not affect the optical transparency.

Moreover, the samples were electrically characterized. The PANI–PSS film had an electrical conductivity of $1.4 \times 10^{-2}$ S/cm, which increased by two orders of magnitude and reached a value of 1.31 S/cm after the DMSO modification. Until now, the mechanism of the observed conductivity enhancement was under study.

The devices with PANI–PSS and DMSO-doped PANI–PSS HILs were compared to the one fabricated directly on ITO, and they showed the best electrical characteristics (Fig. 6), the lowest turn-on voltage (from 5 to 2.5 V; Fig. 7), and enhanced efficiency (Fig. 8). In particular, as shown in Figure 6, the current of the device with ITO/DMSO-doped PANI–PSS was higher with than that of the ITO/PANI–PSS based device until 6.5 V, even though it was not easily distinguishable because the data were reported in log–log scale. This increase was due to the increase of the leakage currents. These currents were due to the agglomerates generated by DMSO-doping, which increased the roughness and partially activated undesired current paths and increased the electrical noise, as observed at 4–5 V. Because the leakage currents had a linear behavior, their contribution became less significant with respect to the device current, which had a power law behavior as the voltage further increased.

Furthermore, the device efficiency grew about two times with the introduction of the DMSO-doped PANI–PSS film (0.77 Cd/A) and about three times with the introduction of the PANI–PSS layer (1.20 Cd/A) in the OLED structure, which without HIL, had a lower efficiency (0.4 Cd/A).

By including an higher conductive film, such as a doped PANI–PSS layer, to an OLED device structure, an efficiency increase is not necessary implied. The potential causes of a decrease in the device efficiency can be the aforementioned HIL roughness, to the further unbalance of the hole-electron pairs, and the modification of the energy levels at the ITO/HIL and HIL/HTL interfaces.[31]

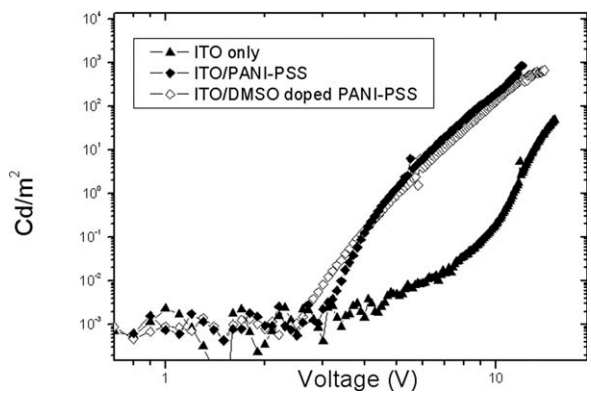


**Figure 7** EL curves of the devices with ITO/PANI–PSS, ITO/DMSO-doped PANI–PSS, and only ITO.

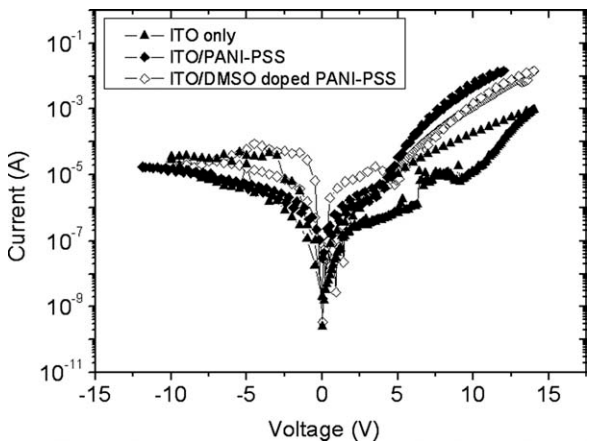


**Figure 9** *I–V* characteristics of three devices under testing in forward and reverse bias.

By following these considerations and observing the current–luminance curves of all devices (Fig. 7), we found it possible to understand the luminance decrease detected in the device with DMSO-doped PANI–PSS.[32] This indicated that the right HIL was not necessarily the more conductive film.

In Figure 9, it is possible to observe the *I–V* plot of the three devices under testing, with both the forward bias and the reverse bias to analyze a potential hysteresis behavior and to determine information on the electrical stability and the rectification ratio.

The device with only ITO showed a strong hysteresis behavior, both in the forward and reverse biases, and the device with ITO/DMSO-doped PANI–PSS was characterized by the same behavior, mainly in the reverse bias. Differently, the device with ITO/PANI–PSS was more stable and had no significant hysteresis behavior. As reported in the literature, this behavior could be attributed to the presence of parasitic currents generated by the ITO spikes.[33]

The presence of the PANI–PSS layer seemed to reduce this effect but not completely when PANI–PSS was DMSO-doped. Moreover, the device with the undoped PANI–PSS layer was characterized by the highest rectification ratio. Indeed, in this case, the forward current was the highest one, and the reverse current was the lowest one.

These results show that the device with PANI–PSS was the more suitable one to be used as an HIL in an OLED device, and the doping of PANI–PSS provided no benefit to the OLED device.

## CONCLUSIONS

Water-dispersed PANI–PSS was synthesized by chemical oxidation polymerization in the presence of excess HCl, and the corresponding films were used as an HIL to improve the performance of OLED devices. The obtained films were homogeneous with a low surface roughness (ca. 10–13 nm) and transparent (transmittance $\approx$ 84%) and had an electrical conductivity of about $1.4 \times 10^{-2}$ S/cm. The film conductivity improved two orders of magnitude, reaching a value of 1.31 S/cm with the addition of DMSO. The device with undoped PANI–PSS showed the best electrical characteristic, the lower turn-on voltage (2.5 V), and improved efficiency, three times that of the device without an HIL.

Further investigations to explain the variation of the mechanisms of the hole-injection and the involved energy levels at the HIL/HTL interface in OLED devices can be assessed in the future through spectral impedance measurements.

## References


1. Yu, H. Y.; Feng, X. D.; Grozea, D.; Lu, Z. H.; Sodhi, R.; Hor, A. M. Appl Phys Lett 2001, 78, 2595.
2. Liu, G.; Kerr, J. B.; Johnson, S. Synth Met 2004, 144, 1.
3. Ohta, H.; Orita, M.; Hirano, M.; Hosono, H. J Appl Phys 2002, 91, 3547.
4. Leterrier, Y.; Medico, L.; Demarco, F.; Manson, J. A.; Betz, U.; Escola, M. F. Thin Solid Films 2004, 460, 156.
5. VanSlyke, S. A.; Chen, C. H.; Tang, C. W. Appl Phys Lett 1996, 69, 2160.
6. Kurosaka, Y.; Tada, N.; Ohmori, Y.; Yoshino, K. Jpn J Appl Phys 1998, 37, L872.
7. Hu, W.; Manabe, K.; Furukawa, T.; Matsumura, M. Appl Phys Lett 2002, 80, 2640.
8. Qiu, C. F.; Chen, H. Y.; Xie, Z. L.; Wong, M.; Kwok, H. S. Appl Phys Lett 2002, 80, 3485.
9. Kim, S. Y.; Lee, J.-L.; Kim, K.-B.; Tak, Y.-H. Appl Phys Lett 2005, 86, 133504.
10. Hsu, C. M.; Wu, W. T. Appl Phys Lett 2004, 85, 840.
11. Nuesch, F.; Carrara, M.; Schaer, M.; Romero, D. B.; Zuppiroli, L. Chem Phys Lett 2001, 347, 311.
12. Yang, Y.; Heeger, A. J. Appl Phys Lett 1994, 64, 1245.
13. Elschner, A.; Bruder, F.; Heuer, H.-W.; Jonas, F.; Karbach, A.; Kirchmeyer, S.; Thurm, S. Synth Met 2000, 111, 139.
14. Shen, Y.; Jacobs, D. B.; Malliaras, G. G.; Koley, G.; Spencer, M. G.; Ioannidis, A. Adv Mater 2001, 13, 1234.
15. Gyoutoku, A.; Hara, S.; Komatsu, T.; Shirinashihama, M.; Iwanaga, H.; Sakanoue, K. Synth Met 1997, 91, 73.
16. Jiang, H.; Zhou, Y.; Ooi, B. S.; Chen, Y.; Wee, T.; Lam, Y. L.; Huang, J.; Liu, S. Thin Solid Films 2000, 363, 25.
17. Shirota, Y.; Kuwabara, Y.; lnada, H.; Wakimoto, T.; Nakada, H.; Yonemoto, Y.; Kawami, S. Appl Phys Lett 1994, 66, 807.
18. Hsu, C.-M.; Wu, W.-T. Appl Phys Lett 2004, 85, 840.
19. Chan, I. M.; Hong, F. C. Thin Solid Films 2004, 450, 304.
20. Choi, H. J.; Cho, M. S.; Kim, J. W.; Kim, C. A.; Jhon, M. S. Appl Phys Lett 2001, 78, 3806.
21. Liu, W.; Kumar, J.; Tripathy, S.; Senecal, K. J.; Samuelson, L. J Am Chem Soc 1999, 121, 71.
22. MacDiarmid, A. G.; Epstein, A. J. Synth Met 1994, 65, 103.
23. Ouyang, J.; Chu, C.-W.; Chen, F.-C.; Xu, Q.; Yang, Y. Adv Funct Mater 2005, 15, 203.
24. Crispin, X. J Polym Sci Part B: Polym Phys 2003, 41, 2561.
25. Wang, G.-F.; Tao, X.-M.; Xin, J. H. Nanoscale Res Lett 2009, 4, 613.
26. MacDiarmid, A. G.; Epstein, A. J. Synth Met 1995, 69, 85.
27. Jang, J.; Ha, J.; Kim, K. Thin Solid Films 2008, 516, 3152.
28. Jang, J.; Ha, J.; Cho, J. Adv Mater 2007, 19, 1772.
29. Chen, S. F.; Wang, C. W. Appl Phys Lett 2004, 85, 765.
30. Petrosino, M.; Vacca, P.; Miscioscia, R.; Nenna, G.; Minarini, C.; Rubino, A. Proc SPIE-Int Soc Opt Eng 2007, 6593, 659310.
31. Vacca, P.; Petrosino, M.; Miscioscia, R.; Nenna, G.; Minarini, C.; Della Sala, D.; Rubino, A. Thin Solid Films 2008, 516, 4232.
32. Kim, K.-B.; Tak, Y.-H.; Han, Y.-S.; Baik, K.-H.; Yoon, M.-H.; Lee, M.-H. Jpn J Appl Phys 2003, 42, L438.